

PHYSICAL CHEMISTRY OF NANOCCLUSERS
AND NANOMATERIALS

The Structural-Phase State of C₆₀–C₇₀ Fullerene Mixtures

M. A. Eremina^a, R. M. Nikonova^a, V. I. Lad'yanov^a, and V. V. Aksenova^b

^a Physicotechnical Institute, Ural Division, Russian Academy of Sciences, ul. Kirova 132, Izhevsk, 426000 Russia

^b Udmurt State University, Krasnoarmeiskaya ul. 71, Izhevsk, 426034 Russia

e-mail: mrere@mail.ru

Received August 4, 2008

Abstract—The structural and phase state of the C₆₀–C₇₀ system at various C₆₀/C₇₀ ratios in mixtures obtained by the vaporization of solutions in toluene at ~98°C was studied by X-ray structure analysis, differential scanning calorimetry, and infrared spectroscopy. Solid solutions based on the face-centered cubic packing of C₆₀ are not formed in the C₆₀–C₇₀ system at C₇₀ contents from 0.5 to 50 wt %. The hexagonal close packing of a solid solution of C₆₀ in C₇₀ can be formed as a result of the thermally activated decomposition of the ternary crystal solvate in the C₆₀–C₇₀–C₆H₅CH₃ system. The structural state of multiphase mixtures formed under conditions far from equilibrium is characterized by a high degree of structure imperfection and greater ability to undergo oxidation compared with C₆₀ and C₇₀.

DOI: 10.1134/S0036024409110193

INTRODUCTION

The existence of solid solutions of C₆₀ in C₇₀ and C₇₀ in C₆₀ is currently questionable and poorly studied. The possibility of their formation is to a substantial extent determined by the sample preparation procedure. In [1], unlimited solubility in the C₆₀–C₇₀ system was observed for samples prepared by sublimation, whereas there was no solubility of C₇₀ over the concentration range 0.04–0.95 wt % when the samples were obtained from solution. The authors of [2–5], however, observed the formation of solid solutions in crystallization from solvents. These solid solutions were based on the face centered cubic packing of C₆₀ with up to 30% C₇₀ [2] and hexagonal close packing at higher C₇₀ concentrations.

According to [3], the introduction of C₇₀ into C₆₀ should result in the appearance of stresses and defects in the lattice and an increase in structure disordering. It was found in [6] that oxygen molecules interacted with defects in fullerene crystallites. The intercalation of molecular gases, in particular, oxygen, is diffusion-controlled and begins already at room temperature [6–10]. Diffusion can occur over bulk defects at crystallite boundaries [6]. This makes diffusion and intercalation/deintercalation processes dependent on the specific surface area of grain boundaries and the concentration of bulk defects. Oxygen intercalated in fullerenes is very difficult to remove without at least insignificant fullerene oxidation [6].

C₆₀–C₇₀ mixtures were found to be more sensitive to oxidation than the pure components. Oxidation involves the formation of C–O–C epoxide bonds, which causes an insignificant weight increase [11], and then carbonyls C=O, whose appearance is related to the destruction of fullerene frameworks [12] with

decomposition to CO and CO₂ [13] and substantial weight loss. According to [14], C₆₀ (99.5%) samples lose only ~1 wt % during annealing in air at 300°C for 24 h and 90 wt % C₆₀ + 10 wt % C₇₀ mixtures lose ~5 wt %; mixtures prepared by the extraction of a solution of fullerene soot in toluene lose as much as 40 wt %, and the residue contains ~16.7 wt % O₂ [14]. The reason for different behaviors of pure fullerenes and their mixtures remains unclear.

In studies of the possibility of formation of C₆₀–C₇₀ solid solutions, changes in fullerene lattice parameters are of importance. Already after the intercalation of molecular gases, the parameter of the face centered cubic lattice of pure fullerene C₆₀ can reach values such as $a = 14.19\text{--}14.25 \text{ \AA}$ [15]. According to [16], $a = 14.185 \text{ \AA}$ for C₆₀O epoxide at room temperature. At the same time, the fullerene lattice parameter can increase to ~14.29 Å also in heating in a vacuum to ~630°C [17]. An increase in the lattice parameter of C₆₀ after thermal treatment in a vacuum at 700°C ($a = 14.72 \text{ \AA}$) was explained [18] by the possibility of intercalation of fullerene fragments into the C₆₀ fullerene lattice.

We showed in [4] that the samples prepared by fairly rapid (~24 h) vaporization of toluene from solutions of fullerenes at room temperature were at least two-phase mixtures consisting of face centered cubic fullerene C₆₀ with the lattice parameter $a = 14.187 \pm 0.010 \text{ \AA}$ (this parameter did not change as the concentration of C₇₀ in C₆₀–C₇₀ mixtures increased from 0 to 50%) and one or two crystal solvate phases depending on mixture composition. The decomposition of crystal solvates led to the formation of a solid solution with hexagonal close packing. At the same time, preliminary measurements showed that the face centered

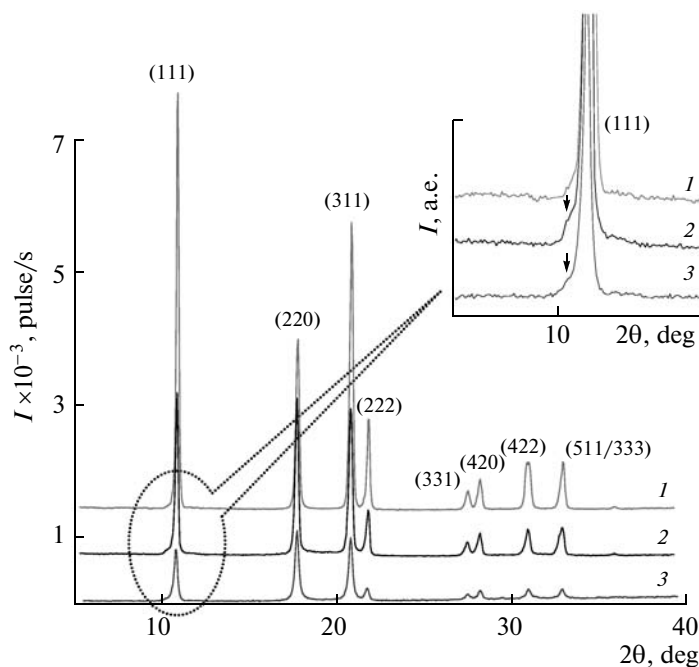


Fig. 1. Diffractograms of C₆₀: (1) reference sample (black powder), (2) reference sample after rapid recrystallization in a vaporizer (black powder), and (3) reference sample after mechanical grinding in a mortar (brown powder).

cubic lattice parameter of C₆₀ increased to $14.23 \pm 0.01 \text{ \AA}$ (this parameter was determined from the last well defined diffractogram line (333)) when a C₆₀—20 wt % C₇₀ mixture was prepared by electric arc synthesis followed by the extraction of fullerenes from fullerene soot by boiling toluene vapors. Possible reasons for such a parameter value can be the formation of a solid solution of C₇₀ in face centered cubic C₆₀ during rapid vaporization of toluene at elevated temperature, the presence of molecular gases (primarily, oxygen) in fullerene crystals [15], oxidation [16], etc.

In view of these findings, it is of interest to study the influence of the conditions of fullerene crystallization from solution on its structural and phase state.

EXPERIMENTAL

In this work, we studied the possibility of formation of solid solutions in the C₆₀-C₇₀ system for the example of model samples containing 0, 0.5, 1, 3, 5, 7, 10, 15, 20, 25, 50, 95, and 100 wt % C₇₀. The samples were prepared by evaporation of solutions in toluene at $\sim 98^\circ\text{C}$ in a 10^{-1} – 10^{-2} atm vacuum. The structural-phase state and composition of the samples were analyzed by X-ray structure analysis, differential scanning calorimetry, and infrared Fourier transform spectroscopy. X-ray measurements were performed on a DRON-6 unit with a graphite monochromator using CuK_α radiation over the angle range 5° – 40° . The differential scanning calorimetry data were obtained on a Diamond DSC (PerkinElmer) instrument in Al crucibles; the samples were heated from -50 to 220°C at a

rate of 20 K/min in a flow of argon. The IR spectra were recorded for samples pressed into pellets with KBr (250 : 1) on a FSM 1202 instrument (14 scans, resolution 1 cm^{-1}). Binary mixture samples were prepared by mixing and complete solution in toluene of os. ch. (special purity) grade of reference C₆₀ (99.95%) and C₇₀ (98%)¹ specimens. The solutions obtained were crystallized in a vaporizer.

RESULTS AND DISCUSSION

The diffractograms of reference C₆₀ before (curve 1) and after (curve 2) recrystallization in a vaporizer are shown in Fig. 1. The structural state of both samples corresponds to face centered cubic C₆₀. C₆₀ · C₆H₅CH₃ crystal solvate apparently does not form, because it is thermally unstable above 90°C [4]. When C₆₀ samples are prepared at room temperature, a certain amount of the face centered cubic C₆₀ phase crystallized directly from the solution, probably because the rate of C₆₀ · C₆H₅CH₃ solvate formation was lower than the rate of toluene vaporization [4]. At a fairly rapid toluene vaporization, the solution becomes supersaturated with respect to C₆₀, and the formation of face centered cubic C₆₀ crystals can be more favorable thermodynamically than solvate formation. The rate of toluene vaporization and solid phase formation increase substantially as the temperature grows from room to $\sim 100^\circ\text{C}$. Fullerene crystallites obtained at high tem-

¹ Fullerenes C₆₀ and C₇₀ were prepared at the Institute of Organometallic Chemistry, ZAO "Fulleren. tsentr" (Nizhni Novgorod).

Lattice parameters (\AA) of a C_{60} – C_{70} mixture of fullerenes before and after annealing in a vacuum at 200 and 400°C for two hours determined from the (422) and (333) lines and a_0 values obtained by the extrapolation of the dependence of the lattice parameter a on $\cos^2\theta/\sin\theta$ [22–24]

[C_{70}], wt %	Initial			200°C, 2 h			400°C, 2 h		
	(422)	(333)	$a_0 \pm 0.01$	(422)	(333)	$a_0 \pm 0.01$	(422)	(333)	$a_0 \pm 0.01$
0	14.18	14.16	14.19	14.17	14.17	14.17	14.17	14.16	14.17
0.5	14.25	14.23	14.17	14.21	14.19	14.17	14.20	14.19	14.16
1	14.20	14.21	14.19	14.20	14.17	14.18	14.18	14.21	14.17
3	14.20	14.21	14.17	14.20	14.19	14.20	14.20	14.21	14.18
5	14.22	14.23	14.22	14.17	14.21	14.18	14.20	14.21	14.17
7	14.20	14.21	14.18	14.20	14.21	14.18	14.22	14.22	14.17
10	14.22	14.25	14.21	14.20	14.21	14.17	–	–	–
15	14.22	14.25	14.22	14.20	14.21	14.16	–	–	–
20	14.24	14.25	14.21	14.20	14.21	14.19	14.22	14.23	14.19
25	14.20	14.25	14.20	14.20	14.21	14.18	14.18	14.23	14.18
50	14.20	14.25	14.17	14.18	14.21	14.21	14.21	14.23	14.20

peratures can therefore contain many defects. This also increases the probability of retention of residual solvent in micropores at microcrystallite boundaries [8, 19].

The diffractogram of recrystallized C_{60} (Fig. 1, 2) contains a “shoulder” close to the (111) peak of face centered cubic C_{60} . Its presence is evidence of the existence of packing defects [20, 21]. It was also observed in [7] for C_{60} samples intercalated with oxygen. According to [7], molecular oxygen is not bound chemically with C_{60} and is adsorbed on the surface of grain boundaries and pores. After annealing in a vacuum, the shoulder disappears from diffractograms [7]. However, in our experiments, the annealing of recrystallized C_{60} in a vacuum at 200–400°C did not cause the disappearance of the shoulder (see below).

The presence of packing defects as a rule not only causes the appearance of the shoulder but also shifts almost all diffractogram lines to larger or smaller angles. Our studies revealed a large spread of lines with respect to their tabulated positions (up to $\pm 0.04 \text{ \AA}$ at a $\pm 0.01 \text{ \AA}$ accuracy of parameter determination). It follows that the determination of the parameter of the face centered cubic lattice of C_{60} based on one separate far and, especially, near (the error is then especially large) line then becomes unjustified [22].

In [23, 24], the true lattice parameter of a metallic alloy with packing defects was calculated using the a_0 value obtained by the extrapolation of a linear dependence of $a(\text{\AA})$ on $\cos^2\theta/\sin\theta$ ($a = a_0$ at $\theta = 90^\circ$). This function is linear in the majority of cases. It takes into account the error caused by the displacement of the plane of the sample from the goniometer center ($\Delta d/d \sim \cos^2\theta/\sin\theta$), which makes the major contribution to lattice parameter errors [22]. In the absence of packing and other bulk defects, all the experimental points should, to within measurement errors, lie on a

straight line, the extrapolation of which to $\theta = 90^\circ$ gives the true lattice parameter.

The face centered cubic lattice parameters for all the mixture compositions studied containing from 0 to 50 wt % C_{70} calculated using two diffraction lines (422) and (333) and the a_0 values obtained using extrapolation are listed in the table. According to [23, 24], the (422) line should experience the smallest displacement in the absence of other bulk defects. The lattice parameters calculated from the (422) line and a_0 values are in many instances close to each other (to within measurement errors). The $a_0 = 14.19 \pm 0.01 \text{ \AA}$ value for recrystallized C_{60} is larger than the lattice parameter given in the literature, $a = 14.15\text{--}14.17 \text{ \AA}$ [25, 26], which can also be caused by the presence of molecular gases, in particular, oxygen, and various impurities, including C_{70} and toluene.

According to [27], the solubility of C_{60} in toluene at room temperature is higher than the solubility of C_{70} . The solubility of C_{60} decreases from ~ 5 to $\sim 2 \text{ mg/ml}$ and that of C_{70} remains almost unchanged ($1.5\text{--}2 \text{ mg/ml}$) as the temperature increases to 80–90°C. The existence of a maximum of the temperature dependence of C_{60} solubility in toluene at 0–30°C is related to the formation of clathrates [27]. At room temperature, the isothermal crystallization of a solution of fullerenes in toluene causes the formation of $C_{60} \cdot C_6H_5CH_3$ and $C_{70} \cdot C_6H_5CH_3$ crystal solvates, whose thermal stabilities are noticeably different [4]. The decomposition of the former is completed at 80–90°C, and that of the latter, at 180°C. At least two types of solvates are formed in the C_{60} – C_{70} –toluene ternary system, the “low-temperature” solvate (decomposes at 70–85°C) structurally similar to $C_{60} \cdot C_6H_5CH_3$ and the “high-temperature” solvate (decomposes at 170–180°C) similar to $C_{70} \cdot C_6H_5CH_3$ [4]. The decomposition of both solvates leads to predominantly the

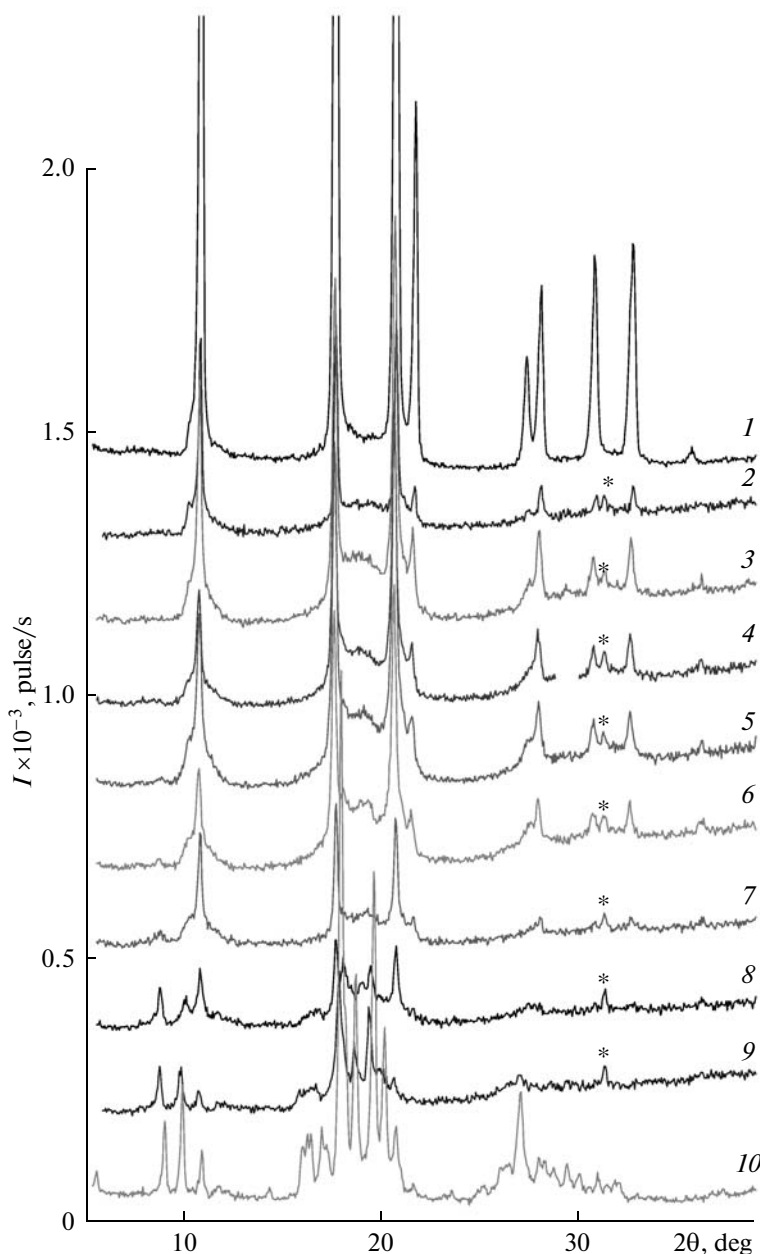


Fig. 2. Diffractograms of freshly prepared C₆₀-C₇₀-C₆H₅CH₃ samples with various C₆₀/C₇₀ ratios: (1) 0, (2) 0.5, (3) 5, (4) 10, (5) 15, (6) 20, (7) 25, (8) 50, (9) 95, and (10) 100 wt % C₇₀; cell material lines are asterisked.

hexagonal closely packed phase. Under the conditions of mixture sample preparation at $\sim 100^\circ\text{C}$, either the formation of the low-temperature crystal solvate in mixtures should not occur or this solvate should decompose immediately.

When C₇₀ is introduced into C₆₀, the structural state of mixtures obtained by recrystallization in a vaporizer is represented by the phase based on face centered cubic C₆₀ and the phase of the high-temperature crystal solvate (Fig. 2). The volume fraction of the crystal solvate phase increases and that of face centered cubic fullerene C₆₀ decreases as the concentra-

tion of C₇₀ in mixtures and solutions grows. This is substantiated by a decrease in the intensity of C₆₀ diffraction lines (Fig. 2). An analysis of the diffractograms presented in Fig. 2 shows that the half-width of face centered cubic C₆₀ fullerene lines increases from $\sim 0.2^\circ$ to $\sim 0.3^\circ$, and the half widths of different lines are different ($\pm 0.03^\circ$).

Line broadening can be caused by a noticeable decrease in the size of blocks (< 100 nm), the presence of packing defects in polycrystalline samples, and microdistortions (crystals with lattice period variations) [28]. All the three factors can play their roles in

the fullerene samples studied by us. Even the addition of as little as 0.5 wt % C_{70} decreases the intensity of face centered cubic C_{60} lines by almost five times, although line widths almost do not increase. A decrease in the intensity of C_{60} lines is caused not only by a decrease in the volume fraction of the phase itself but also by an increase in the number of defects and, likely, mixture dispersity. The introduction of defects into the structure of C_{60} fullerene and a decrease in the mean size of powder particles by approximately five times as a result of mechanical sample grinding in a mortar (according to optical microscope measurements, from ~ 23 to less than $5 \mu\text{m}$) decreases the intensity of diffraction lines, which retain their half-widths, by about 2.5 times (Fig. 1, curve 3), although the lattice parameter remains unchanged ($a_0 = 14.17 \text{ \AA}$).

The presence of a shoulder near the (111) line of face centered cubic C_{60} in the diffraction patterns of initial samples containing 0–25 wt % C_{70} (Fig. 2) leads us to conclude that these samples contain packing defects. The lattice parameter a_0 value ranges from 14.17 to 14.22 \AA (table). Importantly, the position of the shoulder almost coincides with the position of the (111) face centered cubic/(002) hexagonal close packing C_{70} line. No other lines of these phases were, however, observed, although they can nevertheless be present in the samples at the method sensitivity level. They can be characterized by low intensities, and the most intense of these lines can overlap with a “halo” over the range of angles 15° – 23° . The presence of the halo is characteristic of the initial (Fig. 2) and annealed (Fig. 3) mixture sample states and can be caused by the superposition of lines of various phases, including crystal solvate phases (in initial freshly prepared mixtures), C_{70} , C_{60} , fullerene oxides, partially decomposed fullerene molecules, etc.

The annealing of samples at 200–400°C for 2 h in a dynamic vacuum causes the decomposition of the high-temperature crystal solvate [4]. The diffractograms of samples with different contents of C_{70} after annealing at 200°C are shown in Fig. 3 (similar diffractograms were obtained after annealing at 300 and 400°C). If C_{70} is the predominant mixture component (95 and 100 wt % C_{70}), solvate decomposition occurs with the formation of the hexagonal closely packed phase. No separate face centered cubic C_{60} lines were observed for the sample with 5 wt % C_{60} . The hexagonal closely packed lattice parameters of C_{70} were smaller for a mixture ($a = 10.52 \text{ \AA}$ and $c = 17.30 \text{ \AA}$) than for pure C_{70} ($a = 10.55 \text{ \AA}$ and $c = 17.32 \text{ \AA}$), clearly, because of the substitution of part of C_{70} molecules with C_{60} . These results agree with those reported in [2, 4]. A mixture of equal amounts of fullerenes of both types contained both face centered cubic fullerene C_{60} formed during mixture preparation and hexagonal closely packed fullerene $C_{70}(C_{60})$ formed in the decomposition of the high-temperature

solvate $(C_{70}, C_{60}) \cdot C_6H_5CH_3$ [4] with noticeably decreased lattice parameters ($a = 10.43 \text{ \AA}$ and $c = 17.23 \text{ \AA}$). No face centered cubic and hexagonal closely packed C_{70} fullerene lines were observed for samples containing 0.5 to 20 wt % C_{70} because of their low intensities or the absence of these phases. Separate C_{70} lines were present in the diffractogram of the sample with 25 wt % C_{70} , which also contained the halo.

For all the initial mixtures, an increase in the difference between a_0 and the lattice parameter calculated, for instance, from the last line (333) (table) and in the spread of experimental values with respect to the extrapolation dependence of $a(\text{\AA})$ on $\cos^2\theta/\sin\theta$ can qualitatively indicate an increase in the concentration of defects and the degree of structure imperfection as a whole as the content of C_{70} in mixtures increases. We, however, did not observe a monotonic dependence of the lattice parameter a_0 on the content of C_{70} in mixtures. It can be suggested that the solubility of C_{70} in face centered cubic C_{60} is no higher than 0.5 wt %. If the Vegard rule holds, the lattice parameter $\sim 14.17 \text{ \AA}$ should correspond to a 0.4–0.5 wt % content of C_{70} . However, the lattice parameter is already 14.19 \AA for pure C_{60} recrystallized from toluene, and, for this reason, the existence of solubility up to 0.5 wt % C_{70} in face centered cubic C_{60} cannot be determined from changes in the lattice parameter.

Studies of mixtures annealed at 200–400°C showed that there were no changes in the shape and intensity of the shoulder in the small-angle region of the (111) line of face centered cubic C_{60} . Accordingly, it is most probable that packing defects were retained. After annealing, the a_0 parameter of the face centered cubic lattice varied from 14.16 to 14.21 \AA , that is, almost did not change compared with the initial state. The half-width of face centered cubic fullerene C_{60} also remained almost unchanged. After annealing at 200°C for two hours, the difference between a_0 and the a value determined separate lines, for instance, (333) and (422), was insignificant to within measurement errors. Part of defects that caused a substantial spread of diffraction lines of freshly prepared mixtures with respect to the tabulated values was likely caused by just the presence of toluene in the form of crystal solvates or in the free form in micropores and on the surface of microcrystallites [19]; these defects disappeared after annealing, although toluene could be removed not fully. Since the size of pores in fullerene and the size of the toluene molecule do not coincide, the closeness of fullerene packing at the boundary of microcrystals and in micropores is lower in the presence of toluene, and the degree of disordering of such a structure is higher. It is likely that the volume fraction of disordering zones should increase as the size of grains decreases.

Interestingly, after annealing at 400°C, the difference between a_0 and the a parameter determined from separate lines again becomes noticeable (table). It can

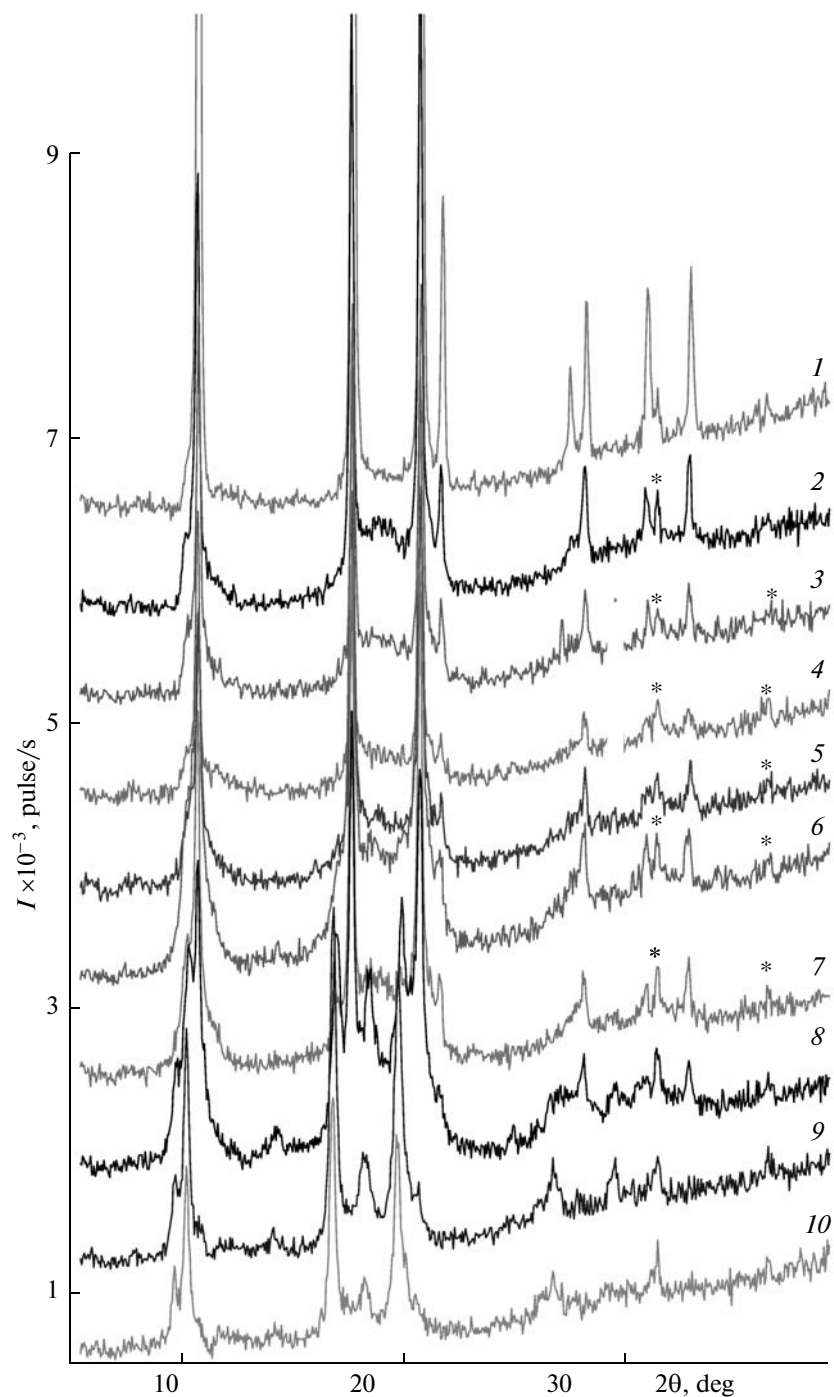


Fig. 3. Diffractograms of C₆₀-C₇₀-C₆H₅CH₃ samples with various C₆₀/C₇₀ ratios after annealing at 200°C for two hours. See Fig. 2 for notation.

be suggested that after annealing in a vacuum for two hours at elevated temperature ($\geq 400^\circ\text{C}$), lattice deformation processes begin, especially if samples contain small amounts of oxygen and solvents. Annealing at a higher temperature (600–700°C) can substantially increase the lattice parameter and cause subsequent crystal structure destruction [18].

IR spectral studies showed that the spectra of samples after annealing in a vacuum at 400°C did not contain absorption bands characteristic of oxides and intermediate stages of the destruction of fullerene molecules, which are characterized by the presence of carbonyl (C=O) groups (Fig. 4). Fragments of C₆₀ and C₇₀ molecule frameworks not bound with oxygen can, however, be present in the samples. The halo in dif-

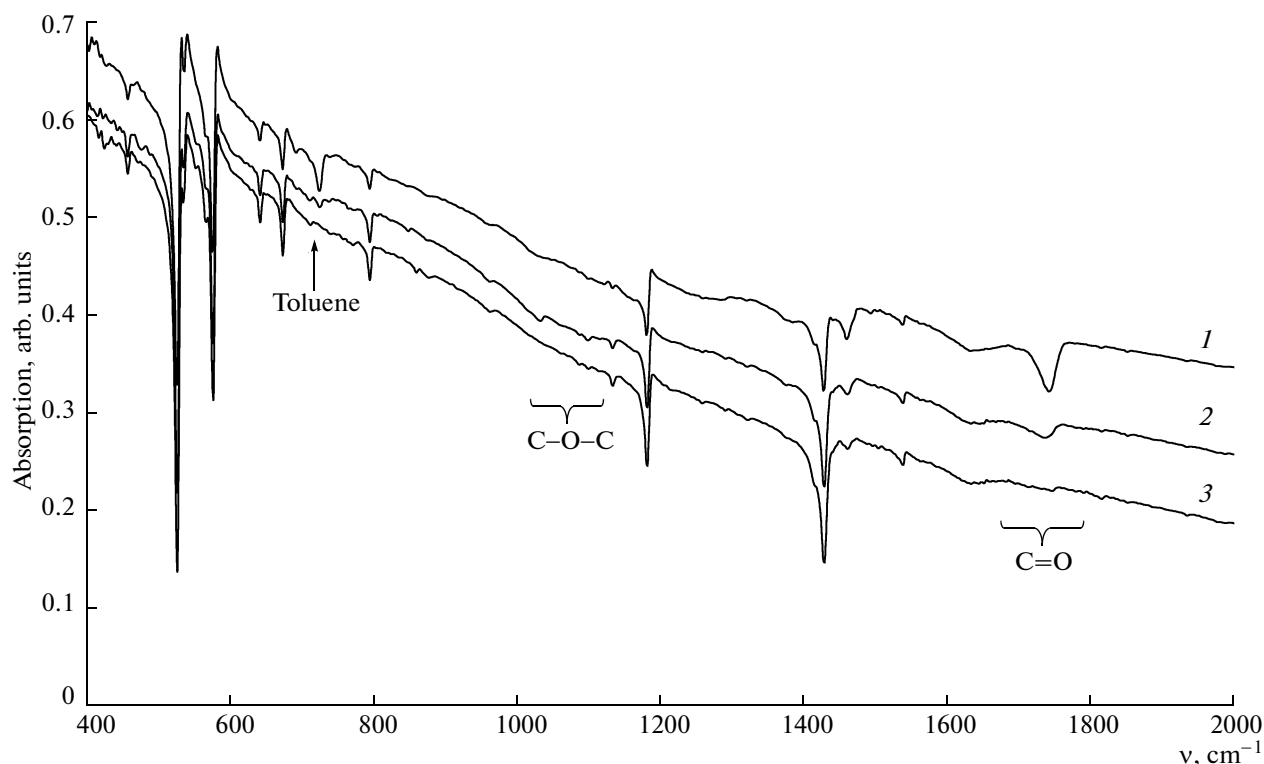


Fig. 4. IR spectra of a mixture of fullerenes (20 wt % C_{70}): (1) initial mixture, (2) mixture after annealing at 200°C for 2 h, and (3) mixture after annealing at 400°C for 2 h in a dynamic vacuum; ν is the wave number.

fraction patterns can then be caused not only by the superposition of substantially broadened fullerene C_{60} and C_{70} phase lines but also by the presence of not oxidized fullerene molecule fragments.

A high degree of structure imperfection of mixture samples is qualitatively substantiated by the differential scanning calorimetry data presented in Fig. 5. The reference C_{60} sample gave an endothermic peak with a maximum at -15.5°C and enthalpy ~ 5.3 J/g, which corresponded to the orientation phase transition (-11 [29], -13 [30], and -15°C [31]). After its recrystallization in a vaporizer, two peaks were observed with maxima at -22°C (enthalpy ~ 4.1 J/g) and -15°C (enthalpy ~ 0.7 J/g). The appearance of the second additional peak in differential scanning calorimetry curves at lower temperatures was primarily caused by the presence of fullerene crystal lattice defects, solid impurities [30], and solvents [19]. The higher the concentration of defects and impurities, the broader the low-temperature differential scanning calorimetry peak and the lower the temperature at which it is observed. In addition, samples obtained by rapid vaporization of a solution in toluene (compared with slow vaporization) also gave two orientation phase transition peaks in differential scanning calorimetry curves.

The rapid vaporization effect is similar to the effect of admixtures of C_{70} to C_{60} (≥ 0.49 wt %). When the solvent is rapidly vaporized, three-dimensional crys-

tals with shifted molecule positions are formed [3]. The low-temperature differential scanning calorimetry peak is characteristic of orientation phase transitions in regions with packing defects, where the distances between the nearest molecules can be larger [32]. It was also reported [19] that, as a result of mechanical grinding of C_{60} and as a consequence of an increase in structure imperfection, the differential scanning calorimetry peak corresponding to the orientation phase transition became broadened, and its temperature decreased; the peak almost disappeared as the duration of grinding increased.

The addition of as little as 0.5 wt % C_{70} to C_{60} caused the complete disappearance of differential scanning calorimetry peaks. At higher concentrations of C_{70} and for pure C_{70} , we did not observe effects corresponding to orientation phase transitions in C_{60} and C_{70} reported in many works, including [31, 33–36]. Annealing of recrystallized mixtures in a dynamic vacuum at 200–400°C did not cause noticeable changes in differential scanning calorimetry curves.

As mentioned above, the presence of structural defects and dispersity of fullerene crystallites to a great extent determine their ability to undergo oxidation. The differential scanning calorimetry data (Fig. 6) show that, during heating in air at a 20 K/min rate, noticeable oxidation and sublimation of the initial recrystallized mixture begin at $\sim 300^\circ\text{C}$, whereas, for

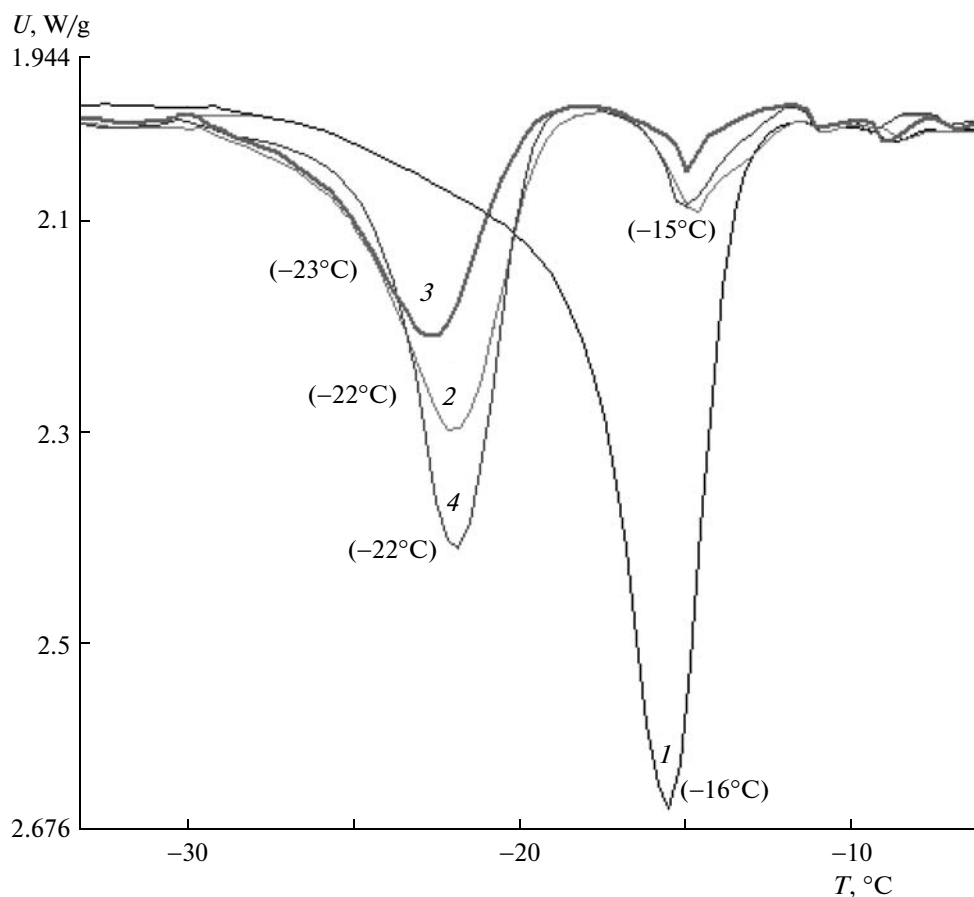


Fig. 5. Differential scanning calorimetry curves for C₆₀: (1) reference sample, (2–4) reference sample after (2) recrystallization and annealing at (3) 200 and (4) 300°C in a vacuum for 2 h (the temperatures corresponding to peak maxima are given in parentheses); *U* is the heat flow.

reference C₆₀ and C₇₀ samples, these processes begin above 450–500°C. At the same time, preliminary annealing in a vacuum at 200°C of mixture samples prepared by recrystallization in a vaporizer followed by heating in air gives the results similar to those obtained for reference samples. The reason for the different behaviors of the samples can be the appearance of impurities during their preparation, such as toluene, oxides, oxygen, the products of the decomposition of fullerenes, etc.

IR spectral studies showed that the reference C₆₀ and C₇₀ samples almost did not contain oxides and oxidized fragments of decomposed fullerene frameworks both before and after recrystallization (Fig. 7). At the same time, both recrystallized reference samples contained toluene. The amount of toluene was noticeably higher in C₇₀ because of the formation of the C₇₀ · C₆H₅CH₃ solvate. After annealing in air at 200°C for two hours, toluene almost fully disappeared from C₇₀ but remained in C₆₀; the same result was obtained in [19]. According to the IR data, there was no noticeable oxidation of the reference samples, which correlated with the differential scanning calorimetry data.

The spectra of recrystallized mixtures (Fig. 4), both prepared from the reference samples and from fullerene-containing soot, contained not only absorption bands of C₆₀, C₇₀, and toluene, but also weak absorption bands of carbonyl groups (C=O) at 1735–1740 cm⁻¹; these bands appeared as a result of the decomposition of fullerene molecules. C–O–C group vibrations at 1030–1100 cm⁻¹ were almost absent. This is evidence that the oxidation and decomposition of fullerenes occur already during the preparation of the samples. The annealing of mixtures at 200°C in a dynamic vacuum (10⁻³–10⁻⁴ atm) results in the almost complete disappearance of toluene from the samples; sometimes, the oxidation of samples occurs, likely with the participation of adsorbed molecular oxygen and molecular oxygen entrapped by fullerene molecules under low vacuum conditions (10⁻¹–10⁻² atm) during preparation. During evacuation, molecular oxygen removal and fullerene oxidation processes compete [19]. Annealing at 400°C in a vacuum allows both oxides and oxidized fullerene molecule fragments to be removed. Importantly, mixture samples preliminarily annealed in a vacuum at 200–400°C and then in air at 200°C almost do not expe-

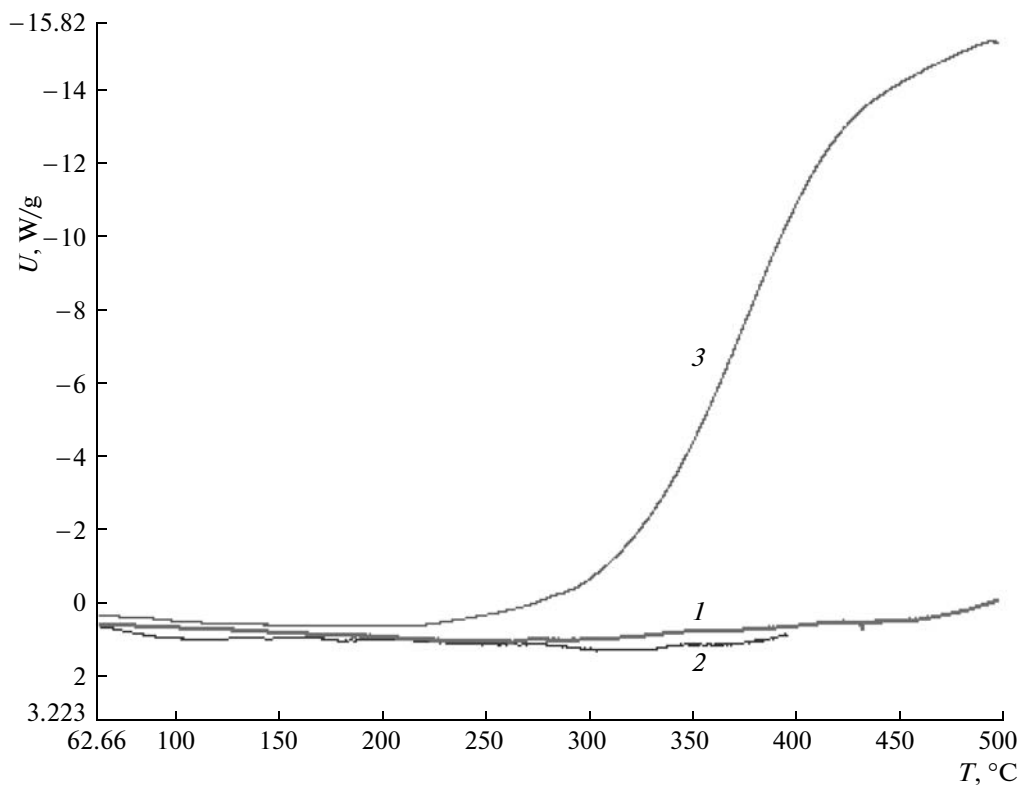


Fig. 6. Differential scanning calorimetry curves: (1) C₆₀ reference sample, (2) C₇₀ reference sample, (3) freshly prepared mixture of fullerenes with 20 wt % C₇₀ obtained by extraction from fullerene soot with toluene. Heating was performed in air at a rate of 20 K/min.

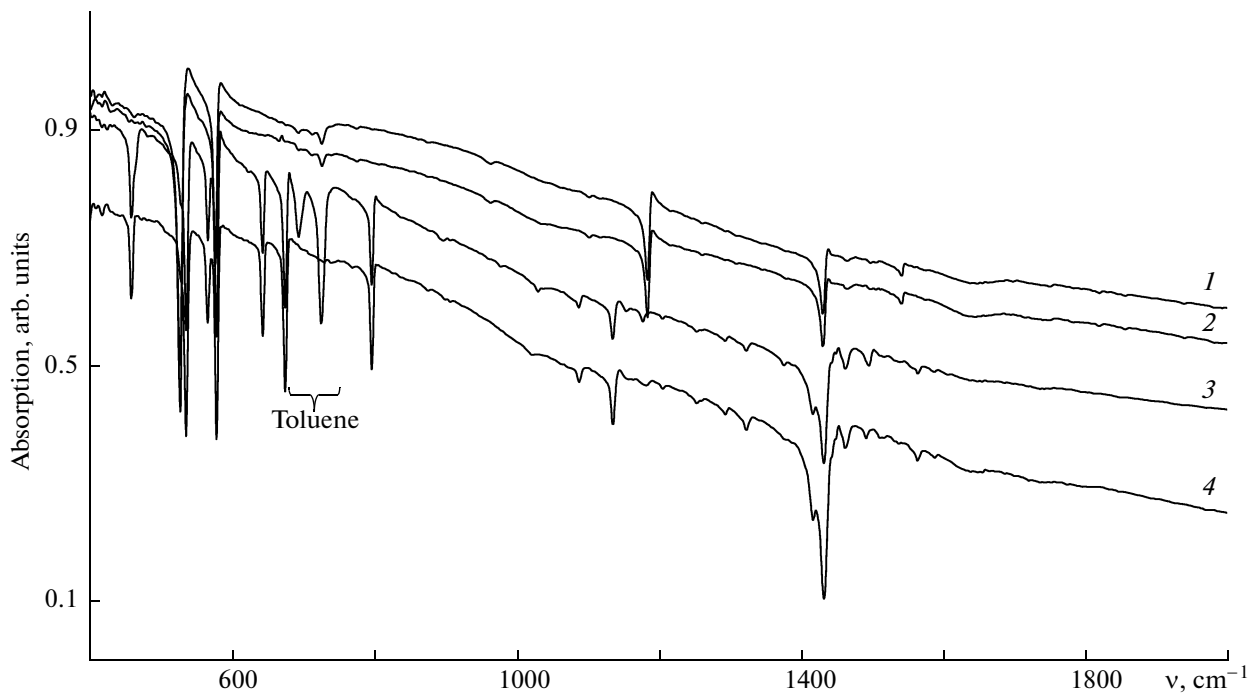


Fig. 7. IR spectra of C₆₀ and C₇₀ reference samples: (1) initial C₆₀, (2) C₆₀ after annealing at 200°C for 2 h, (3) initial C₇₀, and (4) C₇₀ after annealing at 200°C for 2 h.

rience oxidation, as distinct from freshly prepared mixtures, which correlates with the differential scanning calorimetry data.

Other things being equal, the difference in the intensity of oxidation of reference samples and of initial mixtures obtained by recrystallization cannot be directly caused by the presence of residual toluene. The IR data are indicative of its presence in all freshly prepared samples. The oxidized fragments formed in the decomposition of fullerene molecules are retained after annealing in a vacuum at 200°C, and annealed C₆₀-C₇₀ mixtures almost do not undergo oxidation compared with freshly prepared mixtures. For this reason, the intensity of sample oxidation does not strongly depend on the partial destruction of fullerene molecules with the formation of oxidized framework fragments during mixture preparation.

Annealing in a dynamic vacuum at 200°C results in the complete or partial (as with C₆₀) removal of not only toluene but also molecular oxygen [6, 7, 19]. It is likely that the larger the amount of gas impurities in the initial samples, the larger the molecular gas (predominantly, oxygen) fraction that remains during evacuation and low-temperature heating and the higher the intensity of oxidation during thermal treatment at 200°C in a vacuum. Higher structural imperfection and dispersity of recrystallized mixtures are likely accompanied by a more noticeable fraction of molecular oxygen adsorbed initially or diffused deep into crystallites. For this reason, the oxidation of freshly prepared mixtures occurs more intensely than the oxidation of mixtures after annealing or C₆₀ and C₇₀ reference samples prepared similarly.

To summarize, we showed that the preparation of C₆₀-C₇₀ mixtures containing 0.5–50 wt % C₇₀ by the vaporization of boiling solutions in toluene did not cause the formation of face centered cubic solid solutions of C₇₀ in C₆₀. The formation of a hexagonal closely packed solid solution of C₆₀ in C₇₀ is possible as a result of the thermally activated decomposition of the ternary C₆₀-C₇₀-C₆H₅CH₃ crystal solvate. The structural state of multiphase mixtures formed under the conditions far from equilibrium is characterized by a high degree of imperfection and their greater ability to undergo oxidation compared with C₆₀ and C₇₀.

ACKNOWLEDGMENTS

This work was financially supported by the basic research program of the Presidium of Russian Academy of Sciences "Development and Studies of Fullerene-Containing Nanomodifiers."

REFERENCES

1. K. Kniaz, J. E. Fischer, L. A. Girifalco, et al., *Sol. State Commun.* **96**, 739 (1995).
2. Baba M. Sai, T. S. Lakshmi Narasimhan, R. Balasubramanian, et al., *J. Phys. Chem.* **98**, 1333 (1994).
3. D. L. Dorset, *J. Phys. Chem.* **100**, 16706 (1996).
4. M. A. Eremina, V. I. Lad'yanov, and R. M. Nikonova, *Russ. J. Phys. Chem. A* **82**, 2207 (2008).
5. J. Takahashi, *J. Electron. Microsc.* **49**, 719 (2000).
6. M. Wohlers, H. Werner, T. Belz, et al., *Microchim. Acta* **125**, 401 (1997).
7. T. Itoh, S. Nitta, and S. Nonomura, *J. Phys. Chem. Solids* **58**, 1741 (1997).
8. K. Kaneko, C. Ishii, T. Arai, et al., *J. Phys. Chem. Solids* **97**, 6764 (1993).
9. A. Dworkin, H. Szwarc, and R. Ceolin, *Europhys. Lett.* **22**, 35 (1993).
10. H. Werner, D. Bublak, U. Gobel, et al., *Angew. Chem., Int. Ed. Engl.* **31**, 869 (1992).
11. P. K. Gallagher and Z. Zhong, *J. Therm. Anal.* **38**, 2247 (1992).
12. M. Wohlers, H. Werner, D. Herein, et al., *Synth. Met.* **77**, 299 (1996).
13. D. W. McKee, *Carbon* **29**, 1057 (1991).
14. J. C. Scanlon, J. M. Brown, and L. B. Ebert, *J. Phys. Chem.* **98**, 3921 (1994).
15. Yu. M. Shulga, S. A. Baskakov, V. M. Martinenko, et al., in *7th Biennial Intern. Workshop on Fullerenes and Atomic Clusters IWFAC'2005, June 27–July 1* (St. Petersburg, 2005), p. 153.
16. G. B. M. Cox, P. A. Heiney, D. E. Cox, et al., *Chem. Phys.* **168**, 185 (1992).
17. W. Vogel, *Appl. Phys. A* **62**, 295 (1996).
18. C. S. Sundar, A. Bharathi, Y. Hariharan, et al., *Solid State Commun.* **84**, 823 (1992).
19. E. V. Skokan, *Doctoral Dissertation in Chemistry* (RGB, Moscow, 2006).
20. D. Schryvers, G. van Tendeloo, J. van Landuyt, et al., *Meccanica* **30**, 433 (1995).
21. W. Bensch, H. Werner, H. Bartl, et al., *J. Chem. Soc., Faraday Trans.* **90**, 2791 (1994).
22. A. A. Rusakov, *Roentgenography of Metals* (Atomizdat, Moscow, 1977) [in Russian].
23. R. P. I. Adler and C. N. J. Wagner, *J. Appl. Phys.* **33**, 3451 (1962).
24. C. N. J. Wagner, A. S. Tetelman, H. M. Otte, et al., *J. Appl. Phys.* **33**, 3080 (1962).
25. P. C. Chow, X. Jiang, G. Reiter, et al., *Phys. Rev. Lett.* **69**, 2943 (1992).
26. P. A. Heiney, J. E. Fischer, A. R. McGhie, et al., *Phys. Rev. Lett.* **66**, 2911 (1991).

27. V. N. Bezmel'nitsyn, A. V. Elets'kii, and M. V. Okun', *Usp. Fiz. Nauk* **168**, 1195 (1998) [*Phys. Usp.* **41**, 1091 (1998)].
28. V. I. Iveronova and G. P. Revkevich, *Theory of X-rays Scattering* (Mosk. Gos. Univ., Moscow, 1978) [in Russian].
29. G. Pitsi, J. Caerels, and J. Thoen, *Phys. Rev. B* **55**, 915 (1997).
30. A. K. Gangopadhyay, T. Kowalewski, and J. S. Schilling, *Chem. Phys. Lett.* **239**, 387 (1995).
31. A. Dworkin, H. Szwarc, and R. Ceolin, *Europhys. Lett.* **22**, 35 (1993).
32. G. B. M. Vaughan, Y. Chabre, and D. Dubois, *Europhys. Lett.* **31**, 525 (1995).
33. J. de Bruijn, A. Dworkin, H. Szwarc, et al., *Europhys. Lett.* **24**, 551 (1993).
34. C. Meingast, F. Gugenberger, M. Haluska, et al., *Appl. Phys. A* **56**, 227 (1993).
35. E. Grivei, B. Nysten, M. Cassart, et al., *Phys. Rev. B* **47**, 1705 (1993).
36. T. Tanaka and T. Atake, *J. Phys. Chem. Solids* **57**, 277 (1996).